COMPUTED TOMOGRAPHY

CrossMark

Impact of dual-energy CT post-processing to differentiate venous thrombosis from iodine flux artefacts

Jakob Weiss[1] · Christoph Schabel[1] · Ahmed E. Othman[1] · Georg Bier[2] · Konstantin Nikolaou[1] · Fabian Bamberg[1] · Malte N. Bongers[1]

Abstract

Objectives To investigate the accuracy of dual-energy (DE) CT-based iodine maps (IM) and noise-optimised monoenergetic extrapolations (MEI+) at 40 keV for the detection and differentiation of venous thrombosis (VT) from iodine flux artefacts (IFA) in comparison to portal-venous phase CT (CT_{PV}).

Methods Ninety-nine patients were enrolled in this study. In all patients, VT or IFA was suspected on contrast-enhanced CT and confirmed by follow-up CT or colour-coded ultrasound. All examinations were performed on a third-generation dual-source CT system in DE mode during portal-venous phase. CT_{PV}, IM and 40-keV MEI+ were reconstructed and independently evaluated by two radiologists for the presence/absence of VT and/or IFA. Diagnostic confidence was rated on a three-point scale (3 = high confidence). Quantitative parameters were obtained by calculating contrast-to-noise ratios (CNRs), iodine content and thrombus volume. Diagnostic accuracy was assessed by calculating receiver operating characteristics (ROC) of CNR.

Results Diagnostic confidence was significantly higher for IM and MEI+ [both 3 (2-3)] compared to CT_{PV} [2 (1-3); $p \leq 0.03$]. ROC analysis revealed significantly higher AUC values and increased sensitivity for IM and MEI+ (AUC = 88%/sensitivity = 79.1% and 86%/73.1%) than for CT_{PV} (75%/61.2%; $p \leq 0.01$). Thrombus volume was significantly higher in MEI+ than in IM and CT_{PV} ($p < 0.001$). CNR of thrombosis was significantly higher in IM [11.5 (8.5-14.5), $p < 0.001$] and MEI+ [10.9 (8.8-15.5), $p < 0.001$] than in CT_{PV} [8.2 (5.8-11.4)]. Iodine quantification revealed significantly lower results in VT than in IFA [0.55 mg/ml (0.23-0.90) and 1.81 (1.60-2.12) mg/ml; $p < 0.001$].

Conclusions IM and MEI+ 40 keV showed significantly higher diagnostic confidence and accuracy for the detection and differentiation of VT from IFA in comparison to CT_{PV}.

Key Points
- *Iodine maps and noise-optimised monoenergetic extrapolations at 40 keV increase diagnostic confidence and accuracy for the detection and differentiation of venous thrombosis from iodine flux artefacts.*
- *Dual-energy post-processing can significantly increase contrast-to-noise ratio and the sensitivity for the diagnosis of venous thrombosis*
- *Iodine load in venous thrombosis is significantly lower than in iodine flux artefacts*

Keywords Venous thrombosis · Diagnostic imaging · Contrast media

---

✉ Christoph Schabel
Christoph.Schabel@med.uni-tuebingen.de

[1] Department of Diagnostic and Interventional Radiology, University Hospital of Tübingen, Hoppe-Seyler-Strasse 3, 72076 Tübingen, Germany

[2] Department of Diagnostic and Interventional Neuroradiology, University Hospital of Tübingen, Hoppe-Seyler-Strasse 3, 72076 Tübingen, Germany

Abbreviations

ADMIRE	Advanced modelled iterative reconstruction algorithm
CT_{PV}	Portal-venous phase computed tomography
IFA	Iodine flux artefact
IM	Iodine maps
MEI+	Monoenergetic extrapolations
VT	Vein thrombosis

Introduction

Venous thrombosis is a clinically relevant diagnosis, which can occur throughout the whole venous system [1]. In particular, oncology patients have an elevated risk for thrombosis with potentially life-threating complications, such as pulmonary embolism [2]. Hence, reliable diagnosis is mandatory for appropriate treatment to reduce morbidity and mortality [3]. However, venous thrombosis is often an incidental finding in patients who underwent computed tomography (CT) examinations not focused on the venous system, such as oncological follow-up examinations in portal-venous phase (CT_{PV}) [4, 5]. Thus, it may remain challenging to accurately differentiate between venous thrombosis and iodine contrast media flux artefacts (IFA), which is caused by inflow of non-contrast enhanced blood [6]. This topic is of clinical relevance because ultrasound is the modality of choice for the diagnosis VT and is often limited by artefacts caused by the patient's constitution and the examined area, e.g. the abdomen and pelvis due to air-filled bowl loops [7, 8].

In this context, recent developments in dual-energy CT (DECT) post-processing may serve as potential solution for a reliable detection of venous thrombosis by calculating iodine maps (IM) and noise-optimised monoenergetic extrapolations (MEI+) [6, 9]. IM allow for iodine quantification [10] and MEI+ at low keV levels promotes iodine-based attenuation with increased contrast-to-noise and signal-to-noise ratios [9]. Some studies have been published indicating the benefit of IM and MEI+ to improve image quality and diagnostic accuracy for pathologies of the portal-venous and arterial vascular system [11–16]. However, limited research has been published evaluating the value of DECT post-processing for the venous system although this is of clinical significance [6, 17].

We hypothesised that calculating IM and MEI+ at 40 keV may help to improve diagnostic confidence and accuracy for evaluating the venous system in the setting of suboptimal and/or inhomogeneous venous contrast enhancement.

Therefore, the objective of this study was to investigate the accuracy of DECT-based iodine maps (IM) and monoenergetic extrapolations (MEI+) at 40 keV for the detection and differentiation of venous thrombosis (VT) from iodine flux artefacts (IFA) in comparison to CT_{PV}.

Materials and methods

The local institutional review board approved this retrospective study of routine clinical data and waived the requirement for written informed consent.

Patient characteristics

From July 2015 to December 2016, the evaluation of the electronic patient reports revealed 122 consecutive oncological patients, who fulfilled the following inclusion criteria: (1) contrast-enhanced CT in the portal-venous phase and had incidental findings of either (2) suspected venous thrombosis or (3) contrast media flux artefacts mimicking a potential thrombosis and (4) of whom follow-up imaging [colour-coded ultrasound ($n = 50$) or venous-phase CT examination ($n = 72$) within 4 weeks] was available to confirm the diagnosis. To ensure a reliable diagnosis, venous-phase CT was performed for suspected thrombosis in the thoracic and abdominopelvic vasculature. If thrombosis was suspected in the cervical or femoral veins, ultrasound was used. 23 patients were excluded due to severe artefacts caused by metallic implants resulting in non-diagnostic image quality of the adjacent vasculature. Thus, 99 patients ($n = 68$ with thrombosis in follow-up; $n = 31$ no thrombosis in follow-up) were included as final study cohort with follow-up imaging serving as the reference standard.

Acquisition parameters and Image reconstruction

All examinations were performed on a third-generation dual-source CT system (Somatom Force; Siemens Healthineers, Erlangen, Germany) in DE mode. Images were acquired in the portal-venous phase 90 s after body-weight adapted contrast agent administration (0.5 gl/kg, Imeron 400; Bracco, Milan, Italy) at a flow rate of 2.0 ± 0.5 ml/s using a dual-syringe power injector (Medrad; Bayer, Leverkusen, Germany) followed by a saline flush (40 ml). All examinations were performed with automatic attenuation-based tube current modulation (CareDose4D). Acquisition parameters were: tube A 90 kV and tube B Sn150 kV with reference tube-current time product of 190 mAs and 95 mAs, respectively. Collimation was 0.6×192 mm, pitch 0.6, and gantry rotation time 0.5 s.

Axial images were reconstructed using an advanced modelled iterative reconstruction algorithm (ADMIRE, strength level 2; Siemens Healthineers) with a medium soft kernel (Qr40d) and a slice thickness and increment of 3 mm. For linear blended images, a mixing ratio of 0.8 (tube A:B) was used to calculate 120 kV equivalent mixed images. IM and noise-optimised MEI+ at 40 keV were reconstructed using commercially available software (syngo.via VB10B; Siemens Healthineers) for DECT post-processing.

Image analysis

All image analyses were performed on a workstation using dedicated DE post-processing software (syngo.via, VB10B; Siemens Healthineers)

Reference standard

The reference standard was established by a radiologist with 7 years (C.S.) of training in vascular and abdominal imaging and based on colour-coded ultrasound or follow-up CT imaging.

Diagnostic confidence

Two readers with 4 (J.W.) and 7 (M.B.) years of experience in CT imaging assessed all reconstructions for the presence/ absence of venous thrombosis or iodine flux artefacts independently. If more than one thrombosis was diagnosed ($n = 3$), only the dominant site was included in the final analysis. In addition, the diagnostic confidence was rated on a three-point Likert scale (3 = high confidence; 2 = moderate confidence; 1 = low confidence). To ensure unbiased reading results, the reading was performed in a random order and both readers were blinded to clinical diagnosis and the localisation of the thrombosis. In addition, the individual reconstructions (CT_{PV}, IM, MEI+) of a single patient were reviewed in different reading sessions with a time interval of at least 6 weeks to reduce recall bias.

Thrombus volume

To evaluate whether the mode of reconstruction affects the detectable thrombus size, the actual volume was estimated by measuring the size in all three spatial dimensions (formula 1). The reliability of the measurement was rated on a three-point Likert scale (3 = excellent reliability; 2 = moderate reliability; 1 = poor reliability).

$$\text{Thrombus volume } [ml^3] = \frac{\text{length [cm]} \times \text{width [cm]} \times \text{height [cm]}}{2} \tag{1}$$

Contrast-to-noise ratio (CNR) and iodine quantification

To obtain quantitative image parameters and calculate the CNR and iodine density, attenuation [Hounsfield units (HU)] / iodine content in the VT and IFA was measured on CT_{PV}, IM and MEI+ by the same two radiologists in consensus. To reduce measurement errors, three individual regions of interest of 1-3 cm^2 ($ROI_{thrombus/artefact1-3}$) were placed within VT or IFA, on three adjacent slices without involving the thrombus/artefact border. Additionally, three ROIs ($ROI_{vessel1-3}$) were placed in the contrast-enhanced vessel adjacent to VT/IFA on the same slices. ROI size and location were kept identical for all reconstructions of a patient. Subsequently, CNR was calculated for the different reconstructions of VT and IFA using the following equation:

$$CNR = \frac{\left(HU_{vessel} - HU_{thrombus/artefact}\right)}{\left(\dfrac{SD_{vessel} + SD_{thrombus/artefact}}{2}\right)} \tag{2}$$

Statistical analysis

All statistical analyses were performed using SPSS Statistics (version 22; IMB SPSS, Armonk, NY, USA). As Shapiro-Wilk test revealed non-normally distributed data, thrombus volume and CNR of VT/ IFA were compared using Wilcoxon signed-rank test for multiple comparisons. Results are given as median with interquartile range *in parentheses*.

Diagnostic accuracy was evaluated by calculating receiver operating characteristic (ROC) curves of the CNR analysis with area under the curves (AUCs) as well as the corresponding 95% confidence intervals (CIs) for CT_{PV} images, IM and MEI+ 40 keV reconstructions.

Subjective measurement reliability of thrombus volume was compared using Wilcoxon signed-rank test.

For inter-reader agreement, Cohen's kappa was calculated and interpreted as follows: $\kappa < 0.2$ poor; $\kappa = 0.2 – 0.4$ fair; $\kappa = 0.4 – 0.6$ moderate; $\kappa = 0.6 – 0.8$ substantial; $\kappa > 0.8$ perfect. A p value of less than 0.05 was considered statistically significant.

Results

DECT-based post-processing and image analysis was performed successfully in all patients. Patient characteristics and radiation doses are provided in Table 1.

Diagnostic confidence

Diagnostic confidence for differentiation of thrombosis from iodine flux artefacts was rated moderate (median 2; range 1 - 3) in CT_{PV} images by both readers. In IM and MEI+ reconstructions, reading scores increased for both readers and both modes of reconstruction indicating a significantly higher diagnostic confidence in comparison to the CT_{PV} images (both medians, 3; range, 2-3; $p = 0.03$ and $p = 0.02$, respectively), whereas no significant differences were found between IM and MEI+ ($p = 0.7$). An image example is provided in Fig. 1. Inter-reader agreement was substantial ranging from 0.6-0.7.

Thrombus volume

The reliability for the measurement of the thrombus volume was rated moderate in CT_{PV} (median, 2; range, 1-3) and excellent in IM and MEI+ 40 keV reconstructions with significantly higher values in comparison to CT_{PV} (IM median, 3; range, 5-5; $p = 0.01$; MEI+ 40 median, 3; range, 4-5; $p = 0.03$) and with a substantial inter-reader agreement of 0.7.

Measured thrombus volume was 2.5 ± 5.7 ml^3 for CT_{PV}, 2.9 ± 6.4 ml^3 for IM and 3.5 ± 8.0 ml^3 for MEI+ with significantly higher values for MEI+ compared to IM and CT_{PV} ($p < 0.001$) while a trend towards higher thrombus volume was found between CT_{PV} and IM ($p = 0.06$).

Table 1 Patient demographics and dose values for the whole-body CT of the 99 subjects included in the analysis

Variables	n / mean ± SD
Patients	99
Age / range (years)	64.0 ± 13.2 / 27-91
Gender (m / f)	48 / 51
BMI	26.8 ± 3.9
Thrombosis in follow-up	
Site of thrombosis	68
- Iliac vein	23
- Femoral vein	19
- Jugular vein	11
- Portal vein	10
- Ovarian vein	2
- Others	3
No thrombosis in follow-up	31
Site of IFA	
- Iliac vein	13
- Femoral vein	7
- Jugular vein	5
- Portal vein	4
- Others	2
Diagnoses	
Melanoma	18
Breast cancer	17
Ovarian cancer	10
Colon carcinoma	13
Gastric cancer	6
Oesophagus cancer	4
Cholangiocellular carcinoma	9
Hepatocellular carcinoma	3
Renal cancer	4
Bladder cancer	3
Oro-pharyngeal cancer	5
Others	7
$CTDI_{vol}$ [mGy]	647 ± 347
DLP [mGy × cm]	23.1 ± 110.5

Data are given ± standard deviation

$CTDI_{vol}$ volume CT dose index, DLP dose-length product, IFA iodine flux artefact

Iodine quantification

Iodine quantification revealed significantly lower amounts of iodine in venous thrombosis [0.55 mg/ml (0.23-0.90)] than in the iodine flux artefacts [1.81 (1.60-2.12) mg/ml; $p < 0.001$].

CNR and ROC analyses

CNR was significantly higher in IM (median, 11.5; range, 8.5-14.5, $p < 0.001$) and MEI+ reconstructions (median, 10.9; range, 8.8-15.5, $p < 0.001$) compared to the CT_{PV} images (median, 8.2; range, 5.8-11.4; see Fig. 2). No significant differences were found in the iodine flux artefacts among IM (median, 5.8; range, 4.6-7.6; $p = 0.2$), MEI+ (median, 5.5; range, 4.4-7.1) and CT_{PV} (media 5.3; range, 3.7-6.7; $p = 0.3$).

ROC analyses of CNR for the differentiation of venous thrombosis and iodine flux artefacts revealed highest values for IM [AUC, 0.88 (0.79-0.94); Youden Index, 0.67] followed by MEI+ [AUC, 0.86 (0.77-0.92); Youden Index, 0.64] and CT_{PV} [AUC, 0.75 (0.65-0.84); Youden Index, 0.53, see Fig. 3). Pairwise comparison of ROC curves showed significantly larger areas under the curve for IM [Difference, 0.12 (0.06-0.19), $p < 0.01$] and MEI+ [Difference, 0.10 (0.02-0.19), $p = 0.01$] in comparison with CT_{pv}, whereas no significant differences were found between IM and MEI+ [Difference, 0.02 (-0.04 to 0.07), $p = 0.52$].

Sensitivity and specificity was [79.1% (67.4-88.1); 87% (66.4-97.2)] for IM, [73.1% (60.9-83.2); 91.3% (72-98.9)] for MEI+ and [61.2% (48.5-72.9); 91.3% (72.0-98.9)] for CT_{PV}.

Discussion

In this study, we investigated the diagnostic value of DECT-based iodine quantification and noise-optimised monoenergetic extrapolations for the detection of venous thrombosis and differentiation from iodine flux artefacts. Our results indicate that DECT post-processing with IM and low-keV MEI+ allows for significantly improved diagnostic confidence and diagnostic accuracy for the detection and differentiation of venous thrombosis from iodine flux artefacts in comparison to CT_{PV}.

These results are of clinical interest, as venous thromboses are often diagnosed as incidental findings, especially in oncological follow-up examinations acquired in portal-venous phase. An inhomogeneous venous enhancement, in particular in the pelvic veins, impedes a reliable differentiation of potential thromboses from iodine flux artefacts. Moreover, the ongoing organisation of the thromboses over time is responsible for rendering therapeutic interventions ineffective, such as thrombolysis, thus requiring an accurate and early diagnosis, ideally within the first 20 days [18, 19]. Furthermore, the CT density of a thrombosis seems to vary [20] and has shown to increase over time [21] with the potential to gain identical attenuation as the surrounding blood, making a reliable diagnosis even more difficult. In these cases, as exemplary shown in Fig. 2, the improved image contrast of IM and MEI+ seems to have the highest value to support an accurate differentiation between thrombosis and iodine flux artefacts with significantly higher accuracy than CT_{PV} images.

Although in many cases no DE post-processing is necessary to establish a final diagnosis, it seems helpful to increase diagnostic confidence in comparison to CT_{PV} images alone, as our analysis revealed significantly higher subjective reading
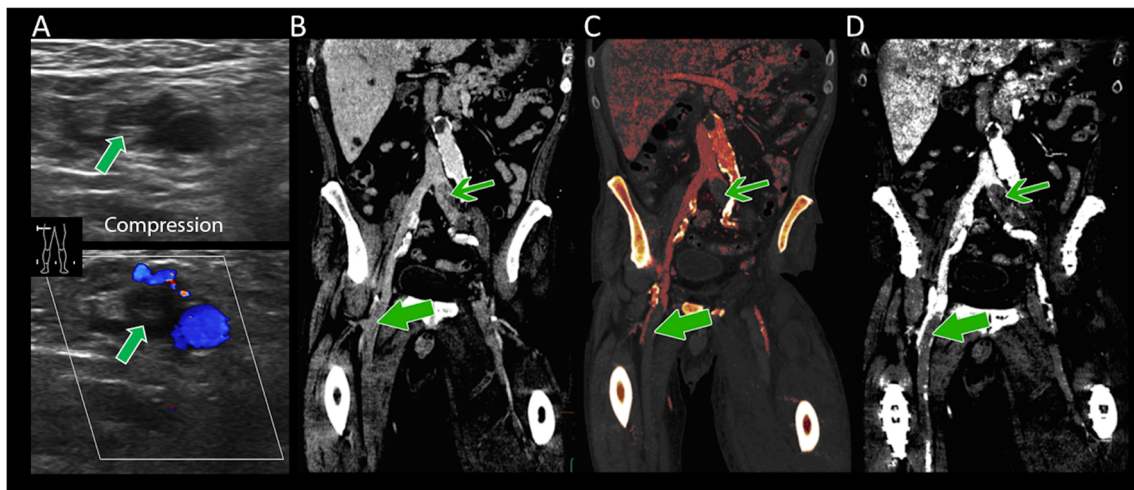
Fig. 1 Ultrasound (**a**) and curved multiplanar reconstructions focused on the on left common iliac and right femoral vein. CT$_{pv}$ images (**b**) revealed thrombosis of the left common iliac vein and inhomogeneous attenuation, but no clear thrombus in the right femoral vein. Iodine maps (**c**) as well as monoenergetic reconstructions at 40 keV (**d**) clearly show an additional thrombosis of the right femoral vein, which could be confirmed with (colour-coded) ultrasound serving as standard of reference

and diagnostic confidence scores for both readers with IM and MEI+ than with the CT$_{PV}$ reconstructions. This may reduce the number of additionally required examinations like ultrasound or CT venography. Although colour-coded ultrasound is a quick and non-invasive method to verify questionable findings in CT examinations of the cervical and lower extremity veins, the diagnostic performance in the thorax as well as in the abdominopelvic region can be limited, e.g. due to gas overlay or obesity [7, 8, 22]. In these cases, CT venography has evolved as a viable diagnostic tool with high sensitivity and specificity due to high iodine load in the venous system, which guarantees a more homogenous enhancement and

consecutively improved contrast of the iodinated blood to the suspected thrombus [23, 24]. However, this procedure requires a second CT examination with additional radiation exposure and intravenous contrast administration [25, 26]. One possibility to compensate for these drawbacks is the use of examination protocols at reduced kVp settings [23, 24]. Due to the closer proximity of the mean photon energy to the iodine k-edge at 33.2 keV, the vascular attenuation can be significantly increased [27, 28]. However, this must be decided in advance and may be at the expense of the image quality of the parenchymal organs. In contrast, the calculation of MEI+ at low keV values provides the same effect and CT$_{PV}$ mixed images allow for optimal assessment of the abdominopelvic organs. Furthermore, the calculation of IM
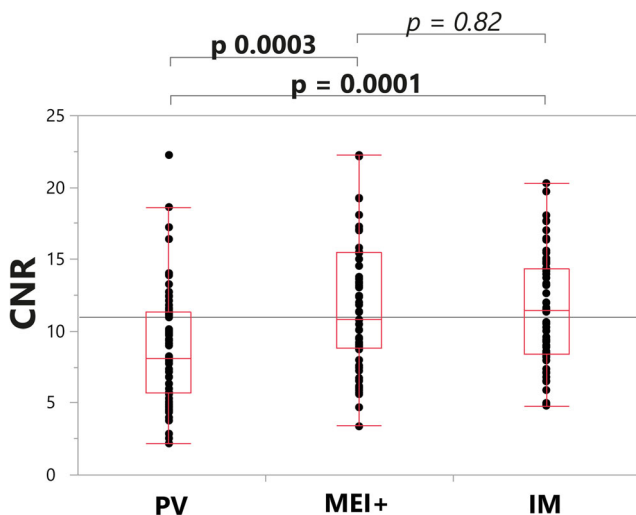

Fig. 2 Box-plots of contrast-to-noise ratio (CNR) values from portal-venous phase CT (PV), monoenergetic extrapolations (MEI+) and iodine mapping (IM) from DECT. CNR of thrombosis increased significantly using IM and MEI+ reconstruction. *Boxes* indicate ranges, *lines within boxes* indicate medians and *vertical lines and whiskers* denote 95% CIs
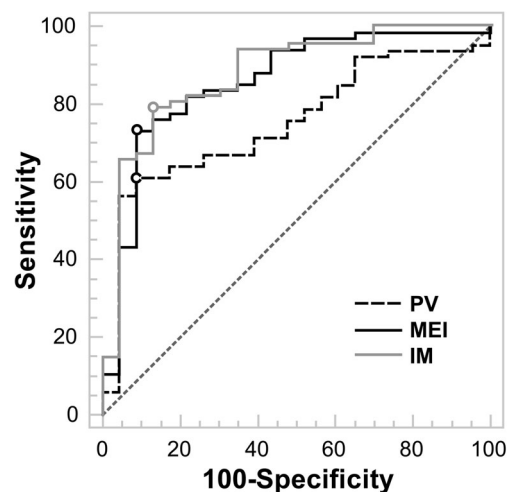

Fig. 3 ROC analysis of CNR from portal-venous phase CT (PV), monoenergetic extrapolation (MEI+) and iodine mapping (IM) from DECT for differentiating between venous thrombosis and iodine flux artefact. The area under the curve was larger for MEI+ and IM than for PV. *Circles* indicate points with highest Youden indices

provides additional information on the quantitative iodine distribution and helps to evaluate questionable results, as previously reported in an ex vivo study [6].

As shown in our quantitative analysis, CNR calculations can support the visual diagnosis to differentiate between venous thrombosis and iodine flux artefacts with highest diagnostic accuracy for iodine maps followed by MEI+. This may be especially helpful if the vessel enhancement is poor or inhomogeneous or if the visual appearance of the finding is questionable due to ill-defined borders or atypical morphology. In these cases, quantitative iodine density measurement may be more accurate than the visual assessment and can serve as an objective decision-making tool.

This study has the following limitations. First, the follow-up interval of 4 weeks is relatively long. However, a new occurrence of a thrombosis at exactly the same location seems rather unlikely. Second, we did not subdivide the thrombosis into non-neoplastic and neoplastic thrombi because the sample size of suspected neoplastic thrombi in our study cohort was too small for a reliable statistical analysis, although neoplastic thrombi may show an increased iodine uptake [11, 12]. In addition, measurement of thrombus volume was only performed in the three evaluated reconstructions (CT_{PV}, MEI+ and IM) and lacks the comparison with the reference standard (venous-phase CT or colour-coded ultrasound), since in most cases no adequate (3D) images of the ultrasound examinations were available in the PACS archive to reliably estimate the thrombus volume. Finally, the retrospective study design is prone to selection bias, which needs to be considered for data interpretation and no information was available, to verify whether or how often DE post-processing was performed in the initial clinical reading.

In conclusion, our results indicate that DE post-processing with IM and MEI+ allows for significantly improved diagnostic confidence and diagnostic accuracy for the detection and differentiation of venous thrombosis from iodine flux artefacts in comparison to CT_{PV} with highest diagnostic confidence and accuracy in the IM reconstructions. This seems particularly useful to rule out a suspected iodine flux artefact rather than to confirm a real venous thrombosis.

Compliance with ethical standards

Guarantor The scientific guarantor of this publication is Malte Bongers.

Conflict of interest The authors of this manuscript declare relationships with the following companies: K. Nikolaou is on the speaker´s bureau of Siemens Healthcare. For the remaining no conflicting interests are declared.

Statistics and biometry No complex statistical methods were necessary for this paper.

Informed consent Written informed consent was waived by the Institutional Review Board.

Ethical approval Institutional Review Board approval was obtained.

Methodology
• retrospective
• diagnostic or prognostic study
• performed at one institution

References

1. Mukai M, Oka T (2018) Mechanism and management of cancer-associated thrombosis. J Cardiol. https://doi.org/10.1016/j.jjcc.2018.02.011
2. Liebman HA, O'Connell C (2016) Incidental venous thromboembolic events in cancer patients: what we know in 2016. Thromb Res 140(Suppl 1):S18–S20
3. Ikushima S, Ono R, Fukuda K, Sakayori M, Awano N, Kondo K (2016) Trousseau's syndrome: cancer-associated thrombosis. Jpn J Clin Oncol 46:204–208
4. Di Nisio M, Ferrante N, De Tursi M et al (2010) Incidental venous thromboembolism in ambulatory cancer patients receiving chemotherapy. Thromb Haemost 104:1049-1054
5. Ageno W, Squizzato A, Togna A et al (2012) Incidental diagnosis of a deep vein thrombosis in consecutive patients undergoing a computed tomography scan of the abdomen: a retrospective cohort study. J Thromb Haemost 10:158–160
6. Bongers MN, Schabel C, Krauss B et al (2015) Noise-optimized virtual monoenergetic images and iodine maps for the detection of venous thrombosis in second-generation dual-energy CT (DECT): an ex vivo phantom study. Eur Radiol 25:1655–1664
7. Karande GY, Hedgire SS, Sanchez Y et al (2016) Advanced imaging in acute and chronic deep vein thrombosis. Cardiovasc Diagn Ther 6:493–507
8. Huisman MV, Klok FA (2013) Diagnostic management of acute deep vein thrombosis and pulmonary embolism. J Thromb Haemost 11:412–422
9. Grant KL, Flohr TG, Krauss B, Sedlmair M, Thomas C, Schmidt B (2014) Assessment of an advanced image-based technique to calculate virtual monoenergetic computed tomographic images from a dual-energy examination to improve contrast-to-noise ratio in examinations using iodinated contrast media. Invest Radiol 49:586–592
10. Chandarana H, Megibow AJ, Cohen BA et al (2011) Iodine quantification with dual-energy CT: phantom study and preliminary experience with renal masses. AJR Am J Roentgenol 196:W693–W700
11. Qian LJ, Zhu J, Zhuang ZG et al (2012) Differentiation of neoplastic from bland macroscopic portal vein thrombi using dual-energy spectral CT imaging: a pilot study. Eur Radiol 22:2178–2185
12. Ascenti G, Sofia C, Mazziotti S et al (2016) Dual-energy CT with iodine quantification in distinguishing between bland and neoplastic portal vein thrombosis in patients with hepatocellular carcinoma. Clin Radiol 71:938.e931–938.e939
13. Wichmann JL, Gillott MR, De Cecco CN et al (2016) Dual-energy computed tomography angiography of the lower extremity runoff: impact of noise-optimized virtual monochromatic imaging on image quality and diagnostic accuracy. Invest Radiol 51:139-146
14. Albrecht MH, Scholtz JE, Husers K et al (2016) Advanced image-based virtual monoenergetic dual-energy CT angiography of the abdomen: optimization of kiloelectron volt settings to improve image contrast. Eur Radiol 26:1863–1870

15. Albrecht MH, Trommer J, Wichmann JL et al (2016) Comprehensive comparison of virtual monoenergetic and linearly blended reconstruction techniques in third-generation dual-source dual-energy computed tomography angiography of the thorax and abdomen. Invest Radiol 51:582–590

16. Weiss J, Notohamiprodjo M, Bongers M et al (2016) Effect of noise-optimized monoenergetic postprocessing on diagnostic accuracy for detecting incidental pulmonary embolism in portal-venous phase dual-energy computed tomography. Invest Radiol 52:142–147

17. Schabel C, Bongers M, Sedlmair M et al (2014) Assessment of the hepatic veins in poor contrast conditions using dual energy CT: evaluation of a novel monoenergetic extrapolation software algorithm. Rofo 186:591–597

18. Stiegler H, Arbogast H, Nees S, Halder A, Grau A, Riess H (1989) Thrombectomy, lysis, or heparin treatment: concurrent therapies of deep vein thrombosis: therapy and experimental studies. Semin Thromb Hemost 15:250–258

19. Kistner RL, Sparkuhl MD (1979) Surgery in acute and chronic venous disease. Surgery 85:31–43

20. Mori H, Hayashi K, Uetani M, Matsuoka Y, Iwao M, Maeda H (1987) High-attenuation recent thrombus of the portal vein: CT demonstration and clinical significance. Radiology 163:353–356

21. Paluch L, Nawrocka-Laskus E, Dabrowska A, Popiela T, Walecki J (2017) Ultrasound elastography for determination of the age of venous thrombi. evaluation of thrombus evolution in patients after sclerotherapy. Pol J Radiol 82:88–91

22. Lim KE, Hsu WC, Hsu YY, Chu PH, Ng CJ (2004) Deep venous thrombosis: comparison of indirect multidetector CT venography and sonography of lower extremities in 26 patients. Clin Imaging 28:439–444

23. Nakaura T, Awai K, Oda S et al (2011) A low-kilovolt (peak) high-tube current technique improves venous enhancement and reduces the radiation dose at indirect multidetector-row CT venography: initial experience. J Comput Assist Tomogr 35:141–147

24. Fujikawa A, Matsuoka S, Kuramochi K et al (2011) Vascular enhancement and image quality of CT venography: comparison of standard and low kilovoltage settings. AJR Am J Roentgenol 197:838–843

25. Loud PA, Katz DS, Bruce DA, Klippenstein DL, Grossman ZD (2001) Deep venous thrombosis with suspected pulmonary embolism: detection with combined CT venography and pulmonary angiography. Radiology 219:498–502

26. Begemann PG, Bonacker M, Kemper J et al (2003) Evaluation of the deep venous system in patients with suspected pulmonary embolism with multi-detector CT: a prospective study in comparison to Doppler sonography. J Comput Assist Tomogr 27:399–409

27. Oda S, Utsunomiya D, Awai K et al (2011) Indirect computed tomography venography with a low-tube-voltage technique: reduction in the radiation and contrast material dose—a prospective randomized study. J Comput Assist Tomogr 35:631–636

28. Cho ES, Chung JJ, Kim S, Kim JH, Yu JS, Yoon CS (2013) CT venography for deep vein thrombosis using a low tube voltage (100 kVp) setting could increase venous enhancement and reduce the amount of administered iodine. Korean J Radiol 14:183–193